Chinese Journal of Natural Medicines

Structurally diverse flavonoids from *Selaginella doederleinii* and their biological activity against laryngeal cancer

Wenqi Liu, Minyu Chen, Sisi Wang, Shiwen Kang, Ni Zheng, Yerlan Bahetjan, Wenting Zhang, Huijian Chen, Xinzhou Yang

Citation: Wenqi Liu, Minyu Chen, Sisi Wang, Shiwen Kang, Ni Zheng, Yerlan Bahetjan, Wenting Zhang, Huijian Chen, Xinzhou Yang, Structurally diverse flavonoids from *Selaginella doederleinii* and their biological activity against laryngeal cancer, Chinese Journal of Natural Medicines, 2026, 24(4), 499−512. doi: 10.1016/S1875−5364(26)61175−2.

View online: https://doi.org/10.1016/S1875−5364(26)61175−2

Chinese Journal of Natural Medicines 24 (2026) 499-512

Contents lists available at ScienceDirect

Chinese Journal of Natural Medicines

journal homepage: www.cjnmcpu.com/

Original article

Structurally diverse flavonoids from *Selaginella doederleinii* and their biological activity against laryngeal cancer

Wenqi Liu[a,Δ], Minyu Chen[a,Δ], Sisi Wang[a], Shiwen Kang[a], Ni Zheng[a], Yerlan Bahetjan[a], Wenting Zhang[b,*], Huijian Chen[a,*], Xinzhou Yang[a,c,d,*]

[a] *International Cooperation Base for Active Substances in Traditional Chinese Medicine in Hubei Province, School of Pharmaceutical Sciences, South-Central Minzu University, Wuhan 430074, China*

[b] *Department of Pharmacy, Tongji Hospital, Tongji Medical College, Huazhong University of Science and Technology, Wuhan 430030, China*

[c] *State Key Laboratory of Drug Research, Shanghai Institute of Materia Medica, Chinese Academy of Sciences, Shanghai 201201, China*

[d] *Xinjiang Key Laboratory of Hetian Characteristic Traditional Chinese Medicine Research, Xinjiang Hetian College, Hetian 848099, China*

ARTICLE INFO

Article history:
Received 13 February 2025
Revised 3 May 2025
Accepted 11 May 2025
Available online 20 April 2026

Keywords:
Selaginella doederleinii
Flavonoids
Cytotoxicity
Laryngeal cancer

ABSTRACT

Ten previously undescribed flavonoids, seladoeflavones J–Q, C, and E (**1**–**10**), together with fifteen known biflavones (**11**–**25**), were isolated from the whole herbs of *Selaginella doederleinii*. The structures of the new compounds were elucidated using 1D and 2D nuclear magnetic resonance (NMR) spectroscopy and mass spectrometry (MS). By comparing experimental spectral data with NMR calculations, the structures of compounds **1**–**5**, **7**, and **8** were assigned. The absolute stereochemistries of compounds **5**–**10** were confirmed by comparing their circular dichroism (CD) spectra with reported data. Notably, the originally proposed structures of seladoeflavones C and E were revised and found to be identical to those of compounds **7** and **8**, respectively. All isolated compounds were evaluated for cytotoxic activity against a panel of cancer cell lines. Most notably, 2'',3''-dihydroochnaflavone (**14**) and involvenflavone G (**19**) exhibited significant anti-proliferative and pro-apoptotic effects in laryngeal cancer cells (Hep-2 and FaDu). Mechanistic studies revealed that compound **14** induced apoptosis by suppressing the protein kinase B (Akt)/mammalian target of rapamycin (mTOR) signaling pathway, whereas compound **19** downregulated endoplasmic reticulum (ER) stress pathways. These findings indicate that compounds **14** and **19** possess strong potential as anti-laryngeal cancer agents, providing robust evidence for the traditional use of *S. doederleinii* in the treatment of laryngeal cancer.

1. Introduction

Currently, laryngeal cancer ranks among the most prevalent malignant tumors, with 184.62 million new cases and 99.84 million deaths reported worldwide in 2020 [1]. Natural products represent a valuable reservoir of structurally diverse compounds exhibiting a wide range of biological activities. Natural compounds used in chemotherapy are often highly effective and less toxic, offering promising alternatives for tumor treatment and holding significant potential for clinical development [2]. Paclitaxel [3], camptothecin [4], and podophyllotoxin [5] have been reported to exhibit significant inhibitory effects against laryngeal cancer. Therefore, the discovery of novel anti-laryngeal cancer agents from natural sources remains a viable strategy to address the growing demand for improved chemotherapeutic options.

The genus *Selaginella* comprises over 700 known species globally, approximately one-tenth of which are native to China [6]. More than 20 species are commonly used in traditional Chinese medicine. Among them, *S. tamariscina* and *S. pulvinata* are officially included in the Chinese Pharmacopoeia 2020 [7]. *S. doederleinii* Hieron. is characterized by a cold nature and bitter taste, contributing to its diverse pharmacological properties, particularly its anti-tumor effects [8]. Medicinal resources of *S. doederleinii* are abundant in southern China. In Chinese Ethnic Medicines, this species is widely employed in the treatment of various cancers, including ovarian, rectal, nasopharyngeal, and lung cancer [9, 10]. The herb and its compound formulations have been clinically applied at Guangxi Folk Hospital for the management of laryngeal cancer and associated complications, demonstrating favorable therapeutic outcomes. Despite its extensive use in *Zhuang* and *Yao* traditional medicine, the active constituents and underlying mechanisms of *S. doederleinii* remain incompletely characterized, leading to a lack of well-defined pharmacodynamic evidence supporting its clinical application. Our previous study first demonstrated that a biflavonoid-rich extract from *S. doederleinii* exerts anti-laryngeal cancer effects through modulation of the IKKβ/NF-κB/COX-2 and protein kinase B (Akt)/Bad signaling pathways [11]. Phytochemical investigations have identified flavonoids, biflavones, alkaloids, lignans, sterols, and other phenolic compounds in *S. doederleinii* [12–14]. In a prior study, we reported the anti-proliferative activity of a new neolignan and six known com-

* Corresponding author.
E-mail addresses: wenting@hust.edu.cn (W. Zhang); 2022066@mail.scuec.edu (H. Chen); xzyang@mail.scuec.edu.cn (X. Yang)
Δ These authors contributed equally to this work.

https://doi.org/10.1016/S1875-5364(26)61175-2

pounds from *S. doederleinii* against laryngeal cancer cells [15]. Over 20 biflavonoids have been isolated from this species, including amentoflavone, robustaflavone, delicaflavone, and ginkgetin, among others. In the present study, we isolated ten new flavonoids, seladoeflavones J–Q, C, and E (**1**–**10**), alongside fifteen known biflavones (Fig. 1). Given that their bioactivities remain insufficiently elucidated, we first evaluated the inhibitory effects of these 25 compounds across four representative cancer cell lines. Notably, they exhibited pronounced inhibitory activity against laryngeal cancer cells. Subsequently, the two most potent compounds with sufficient isolation yields were selected for further evaluation of their effects on laryngeal cancer cell proliferation, invasion, and apoptosis.

Induction of apoptosis is a critical mechanism in anti-cancer therapy. A decreased B-cell lymphoma-2 (Bcl-2)/Bcl-2-associated X protein (Bax) ratio promotes mitochondrial permeability transition pore (MPTP) opening, facilitating the release of cytochrome c (Cyt-c) into the cytosol. Cyt-c associates with apoptotic protease-activating factor-1 (Apaf-1) to form the apoptosome, which activates caspase-9 and subsequently the executioner caspase-3, ultimately triggering apoptosis through DNA fragmentation and loss of plasma membrane asymmetry. Two key regulatory pathways further modulate this process: (1) endoplasmic reticulum (ER) stress: downregulation of glucose-regulated protein 78 (GRP78) impairs unfolded protein binding and disrupts the unfolded protein response (UPR), thereby intensifying ER stress. This leads to activation of pro-apoptotic mediators such as CHOP and JNK, as well as the caspase-4/12-7-3 cascade [16]; and (2) Akt/mammalian target of rapamycin (mTOR) signaling: reduced phosphorylation of Akt and mTOR alleviates their anti-apoptotic effects, thereby promoting mitochondrial apoptosis *via* caspase activation [17]. In this study, we investigated the effects of two bioactive compounds isolated from *S. doederleinii* on these apoptotic pathways, including apoptosome formation, Bcl-2/Bax balance, caspase expression, ER stress, and Akt/mTOR signaling. Our findings provide mechanistic insights into the anti-laryngeal cancer activity of these compounds, underscoring their potential as targeted therapeutic agents.

2. Results and discussion

2.1. Structural elucidation

Seladoeflavone J (**1**) was isolated as a yellow amorphous powder. Its molecular formula was determined to be $C_{22}H_{14}O_8$ based on the pseudomolecular ion peak at *m/z* 407.07602 $[M + H]^+$ (Calcd. for $C_{22}H_{15}O_8$, 407.07614) in the high-resolution electrospray ionization mass spectrometry (HR-ESI-MS) spectrum, corresponding to 16 degrees of unsaturation. The IR spectrum revealed the presence of hydroxyl, carbonyl, and aromatic ring functionalities, as evidenced by absorption bands at 3240, 1651, 1600, 1504, and 1442 cm^{-1}. UV spectral data showed maximum absorption bands at 221, 265, and 345 nm, along with a positive reaction to $AlCl_3$ reagent, which is characteristic of flavonoids [18, 19].

The ^1H nuclear magnetic resonance (NMR) spectrum (Table 1) displayed an AA'BB' coupling system with signals at δ_H 7.82 (2H, d, *J* = 9.0 Hz, H-2', 6') and δ_H 6.88 (2H, d, *J* = 9.0 Hz, H-3', 5'), indicative of a para-substituted benzene ring (ring B). Additionally, two aromatic protons in the A-ring were observed at δ_H 6.54 (1H, d, *J* = 2.1 Hz, H-8) and 6.24 (1H, d, *J* = 2.1 Hz, H-6), along with a low-field hydroxyl signal at δ_H 12.24 (s, 5-OH), which are characteristic of a kaempferol derivative [20]. The ^1H NMR also revealed a para-substituted benzene moiety (ring D) at δ_H 7.15 (2H, d, *J* = 8.9 Hz, H-2'', 6'') and δ_H 7.87 (2H, d, *J* = 8.9 Hz, H-3'', 5''). The ^{13}C NMR and distortionless enhancement by polarization transfer (DEPT) spectra (Table 1) confirmed the presence of 15

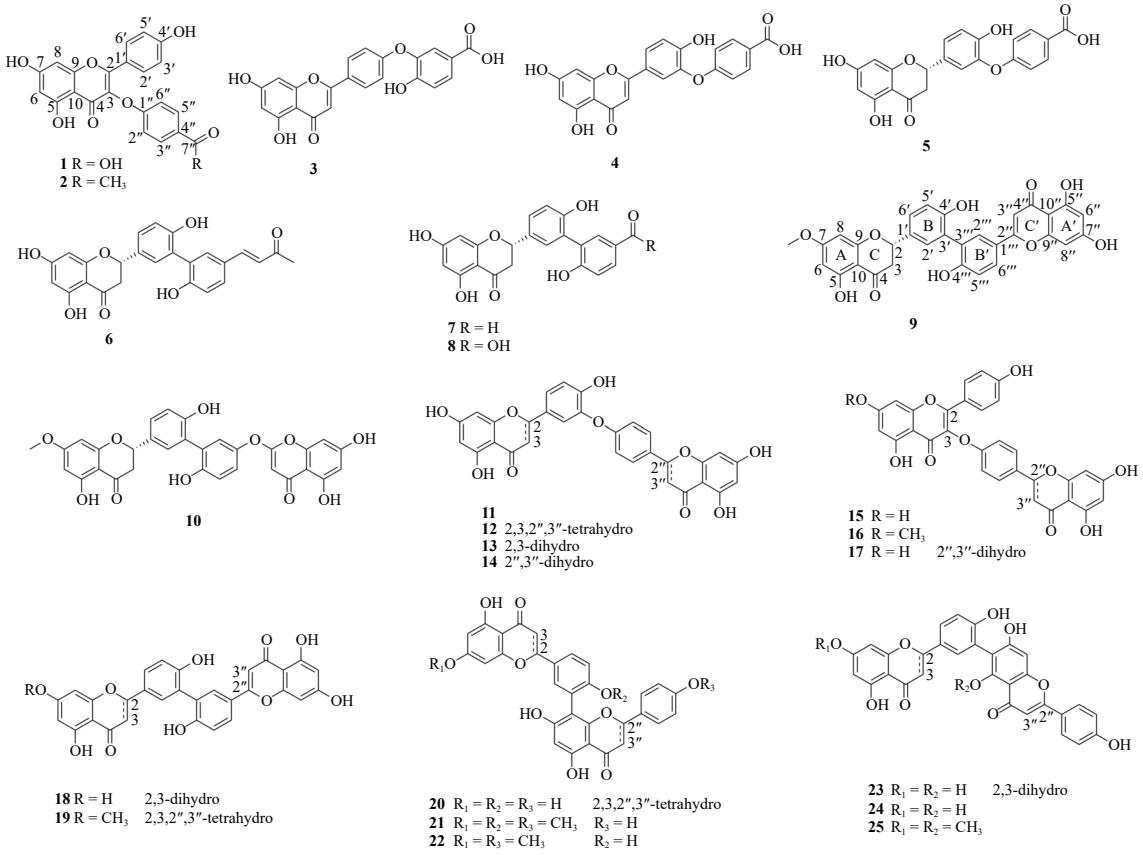

Fig. 1 Structures of compounds **1**–**25**.

Table 1 ^{1}H NMR (600 MHz) and ^{13}C NMR (150 MHz) data for compounds **1**–**3**, kaempferol and apigenin in DMSO-d_6.

No.	**1**		**2**		kaempferol		**3**		apigenin	
	δ_H	δ_C	δ_H	δ_C	δ_H	δ_c	δ_H	δ_c	δ_H	δ_c
2	-	157.0	-	157.0	-	146.8	-	163.0	-	164.8
3	-	131.7	-	131.9	-	135.9	6.87, s	104.1	6.79, s	102.3
4	-	176.0	-	175.9	-	175.9	-	181.8	-	182.1
5	-	161.2	-	161.2	-	159.2	-	161.5	-	161.4
6	6.24, d (2.1)	98.9	6.23, d (2.0)	99.0	6.25, d (2.0)	98.3	6.20, d (2.0)	99.1	6.22, d (2.1)	99.0
7	-	164.6	-	164.9	-	164.0	-	164.6	-	163.3
8	6.54, d (2.1)	94.2	6.53, d (2.0)	94.2	6.49, d (2.0)	93.5	6.49, d (2.0)	94.1	6.53, d (2.1)	94.1
9	-	156.8	-	156.8	-	156.3	-	157.4	-	157.9
10	-	104.2	-	104.0	-	103.1	-	103.7	-	103.7
1'	-	119.7	-	119.7	-	121.8	-	124.5	-	120.6
2'	7.82, d (9.0)	130.2	7.82, d (9.0)	130.2	8.10, d (8.2)	129.5	8.04, d (8.9)	128.5	7.91, d (8.5)	128.8
3'	6.88, d (9.0)	115.8	6.87, d (9.0)	115.8	6.98, d (8.2)	115.4	7.01, d (8.9)	116.5	6.88, d (8.5)	116.1
4'	-	160.7	-	160.7	-	159.2	-	160.7	-	161.2
5'	6.88, d (9.0)	115.8	6.87, d (9.0)	115.8	6.98, d (8.2)	115.4	7.01, d (8.9)	116.5	6.88, d (8.5)	116.1
6'	7.82, d (9.0)	130.2	7.82, d (9.0)	130.2	8.10, d (8.2)	129.5	8.04, d (8.9)	128.5	7.91, d (8.5)	128.8
1''	-	160.1	-	160.3	-	-	-	141.2	-	-
2''	7.15, d (8.9)	115.0	7.17, d (9.0)	115.0	-	-	-	153.7	-	-
3''	7.87, d (8.9)	131.5	7.91, d (9.0)	130.6	-	-	7.08, d (8.5)	117.1	-	-
4''	-	125.0	-	131.6	-	-	7.72, dd (8.5, 2.1)	128.0	-	-
5''	7.87, d (8.9)	131.5	7.91, d (9.0)	130.6	-	-	-	123.3	-	-
6''	7.15, d (8.9)	115.0	7.17, d (9.0)	115.0	-	-	7.56, d (2.1)	123.3	-	-
7''	-	166.8	-	196.4	-	-	-	166.8	-	-
7''-Me	-	-	2.52, s	26.6	-	-	-	-	-	-
5-OH	12.24, s	-	12.23, s	-	-	-	12.87, s	-	12.84, s	-

skeletal carbons from the kaempferol core, with the remaining seven carbons assigned to six aromatic carbons (ring D) and one carbonyl carbon. Heteronuclear multiple bond correlations (HMBCs) of H-3'', 5'' to C-7'' and H-2'', 6'' to C-4'' indicated that the carboxyl carbon at δ_C 166.8 (C-7'') is attached to C-4'' (δ_C 125.0) of ring D (Fig. 2). , suggesting a benzoic acid substituent. Furthermore, the downfield chemical shift of C-1'' (δ_C 160.1), along with HMBCs of H-3'', 5'' and H-2'', 6'' to C-1'', indicated that C-1'' is bonded to an oxygen atom. However, no HMBCs were observed between the kaempferol skeleton and ring D. Comparison of the ^{13}C NMR data of **1** with those of kaempferol under identical conditions revealed significant differences at C-2 and C-3 ($\Delta\delta_C2$ = 10 ppm and $\Delta\delta_{C3}$ = 4 ppm), suggesting a linkage between C-3 and C-1'' *via* an oxygen bridge (C_3–O–$C_{1''}$). To confirm the structure, density functional theory (DFT)-based ^{13}C NMR calculations were performed for three possible frameworks: (C_3–O–$C_{1''}$)-**1**, ($C_{4'}$–O–$C_{1''}$)-**1**, and (C_7–O–$C_{1''}$)-**1**. Using the B3LYP/6-311G(d,p) level and the polarizable continuum model (PCM) in DMSO-d_6, the calculated shifts for (C_3–O–$C_{1''}$)-**1** showed the best agreement with experimental data, supported by a DP4 + probability score of 100.00% (Fig. 3). Its ^{13}C NMR data were able to better match the experimental values, thus providing support for the conclu-

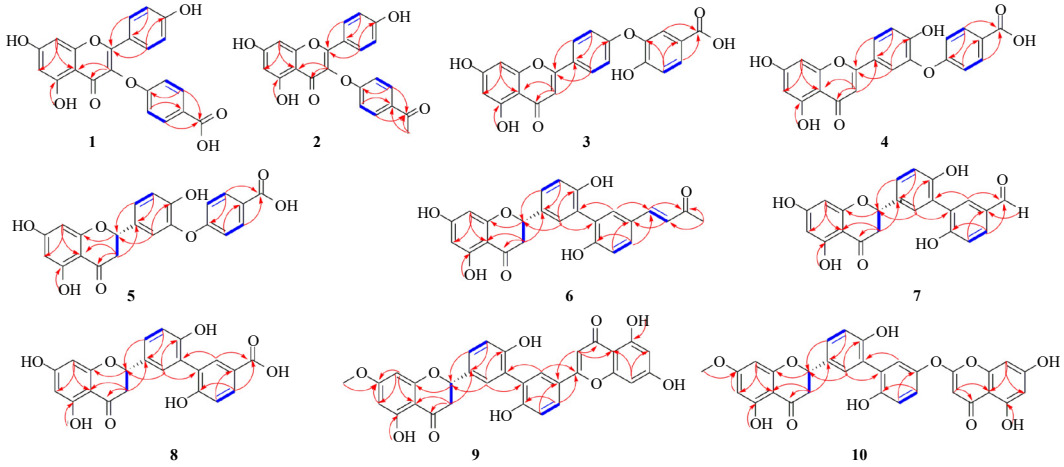

Fig. 2 ^{1}H–^{1}H COSY (–) and key HMBC (→) correlations for compounds **1**–**10**.

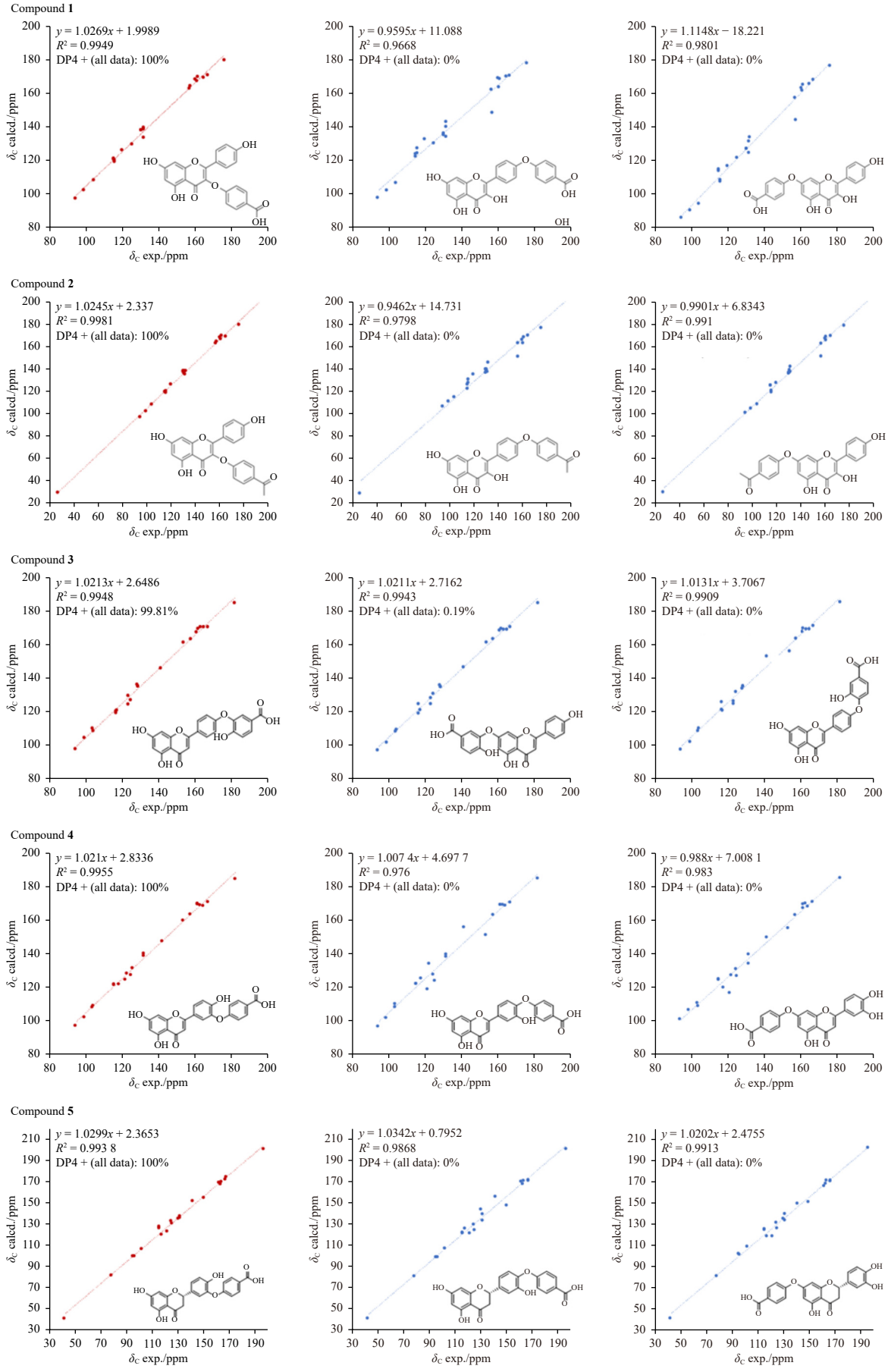

Fig. 3 Linear correlations between the scaled calculated and experimental ^{13}C NMR chemical shifts and statistical DP4 + parameters for compounds **1**–**5**.

sion that the link between kaempferol and the D-ring is *via* C_3-O-$C_{1''}$. Therefore, compound **1** was identified as 4-((5,7-dihydroxy-2-(4-hydroxyphenyl)-4-oxo-4*H*-chromen-3-yl) oxy) benzoic acid, and we named it as seladoeflavone J. Seladoeflavone J stands out as a relatively novel and intriguing example within the diverse family of flavonoids. What makes it particularly distinctive is the unique structural feature where its benzoic acid substituent is connected to C3 *via* a C-O-C bond. This specific linkage not only differentiates it from many other flavonoid derivatives but also suggests the potential for distinct chemical reactivity and biological activities. Such a structural characteristic may offer new insights into the synthesis, modification, and application of flavonoids in various scientific fields, including medicinal chemistry and pharmacology.

Seladoeflavone K (**2**) was obtained as a yellow amorphous powder. Its molecular formula was established as $C_{23}H_{16}O_7$ from the pseudomolecular ion peak at *m/z* 427.078 92 $[M + Na]^+$ (Calcd. for $C_{23}H_{16}O_7Na$, 427.07882) in HR-ESI-MS, indicating 16 degrees of unsaturation. Detailed comparison of the NMR data of **1** and **2** revealed structural similarity, with the key difference being the replacement of the carboxyl group in **1** with an acetyl group at C-4'' of ring D in **2** (δ_C 131.6). This was confirmed by HMBCs of H-3'' (δ_H 7.91), H-5'' (δ_H 7.91), and 7''-Me (δ_H 2.52) to C-7'' (δ_C 196.4), and of H-2'' (δ_H 7.17), H-6'' (δ_H 7.17), and H-7''-Me (δ_H 2.52) to C-4''. The attachment site of ring D was determined by comparison with kaempferol ($\Delta\delta_{C2}$ = 10 ppm, $\Delta\delta_{C3}$ = 4 ppm) and DFT-based ^{13}C NMR calculations for three possible structures: (C_3–O–$C_{1''}$)-**2**, ($C_{4'}$–O–$C_{1''}$)-**2**, and (C_7–O–$C_{1''}$)-**2**. The DP4+ analysis assigned a 100.00% probability to (C_3-O-$C_{1''}$)-**2** (Fig. 3), confirming the C_3–O–$C_{1''}$ linkage. Therefore, compound **2** was identified as 3-(4-acetylphenoxy)-5,7-dihydroxy-2-(4-hydroxyphenyl)-4*H*-chromen-4-one and named seladoeflavone K.

Seladoeflavone L (**3**) was isolated as a yellow amorphous powder, with a molecular formula of $C_{22}H_{14}O_8$ determined by HR-ESI-MS, which showed a pseudomolecular ion at *m/z* 407.075 99 $[M + H]^+$ (Calcd. for $C_{22}H_{15}O_8$, 407.07614). NMR analysis revealed that compounds **1**, **2**, and **3** belong to the biphenyl ether-type (C–O–C) flavonoids, with ring B and ring D connected *via* an oxygen bridge. Compound **3** was identified as an apigenin derivative, characterized by a single proton at δ_H 6.87 (H-3) and an AA'BB' system in ring B at δ_H 8.04 (2H, d, *J* = 8.9 Hz, H-2', 6') and δ_H 7.01 (2H, d, *J* = 8.9 Hz, H-3', 5') [21, 22]. The NMR data also indicated a carboxyl group at δ_C 166.8 (C-7''), located at C-5'' (δ_C 123.3) of ring D, as confirmed by HMBCs of H-4'' (δ_H 7.72), H-6'' (δ_H 7.56) to C-7'', and H-3'' (δ_H 7.08) to C-5''. HMBCs of H-4'' and H-6'' to C-2'' (δ_C 153.7) and of H-3'' and H-6'' to C-1'' (δ_C 141.4) indicated a 1,2,5-trisubstituted benzene ring (ring D). The downfield shift of C-1'' suggested attachment to an oxygen atom. The linkage site was determined by comparison with apigenin ($\Delta\delta_{C1'}$ = 4 ppm) and DFT-based NMR shift calculations. The structure ($C_{4'}$–O–$C_{1''}$)-**3** (Fig. 3) showed the best match with experimental data, indicating that ring D is connected to C-4' (δ_C 160.7) *via* a C–O–C bond. Thus, compound **3** was elucidated as 3-(4-(5,7-dihydroxy-4-oxo-4*H*-chromen-2-yl)phenoxy)-4-hydroxybenzoic acid and named seladoeflavone L.

Seladoeflavone M (**4**) was isolated as a yellow powder. Its molecular formula was determined to be $C_{22}H_{14}O_8$ based on the pseudomolecular ion $[M + H]^+$ at *m/z* 407.075 99 (Calcd. for $C_{22}H_{15}O_8$, 407.076 14) in HR-ESI-MS, indicating 16 degrees of unsaturation, consistent with seladoeflavone L (**3**). In contrast to **3**, the ^{1}H and ^{13}C NMR spectra (Table 2) of **4** exhibited an ABX system in ring B [δ_H 7.88 (1H, overlapped, H-2'), 7.89 (1H, overlapped, H-6'), 7.16 (1H, d, *J* = 8.5 Hz, H-5')], characteristic of a luteolin derivative [23]. Similar to compounds **1**–**3**, the chemical shifts of C-3' (δ_C 141.6) and C-1'' (δ_C 161.2) suggested an oxygen bridge between ring B and ring D. Notably, C-2' and C-3' of **4** showed significant deviations from luteolin ($\Delta\delta_C$ = 8 ppm and 4 ppm, respectively; Table 2), indicating a linkage at C-3'. To confirm the structure, DFT-based ^{13}C NMR calculations were performed for three possible frameworks: ($C_{3'}$-O-$C_{1''}$)-**4**, ($C_{4'}$-O-$C_{1''}$)-**4**, and (C_7-O-$C_{1''}$)-**4**. DP4+ analysis assigned a 100% probability to ($C_{3'}$-O-$C_{1''}$)-**4** (Fig. 3), confirming the linkage. Thus, compound **4** was elucidated as 4-(5-(5,7-dihydroxy-4-oxo-4*H*-chromen-2-yl)-2-hydroxyphenoxy) benzoic acid and named seladoeflavone M.

Seladoeflavone N (**5**) was isolated as a yellow amorphous powder with a specific rotation of $[\alpha]_D^{20}$ −3.97 (*c* 0.42, MeOH). The molecular formula was determined as $C_{22}H_{16}O_8$ from the pseudomolecular ion $[M + H]^+$ at *m/z* 409.091 74 (Calcd. for $C_{22}H_{17}O_8$, 409.091 79) in HR-ESI-MS, indicating two additional hydrogen atoms compared to **4**. 1D and 2D NMR spectra revealed an AMX spin system in the C-ring [δ_H 2.72 (1H, dd, *J* = 17.1, 2.9 Hz, H-3eq), 3.29 (1H, dd, *J* = 17.1, 12.8 Hz, H-3ax), 5.48 (1H, dd, *J* = 12.8, 2.9 Hz, H-2)] and saturated carbon signals at δ_C 78.0 and 42.0, indicating a dihydroflavonoid structure. HMBC, ^{1}H–^{1}H correlation spectroscopy (COSY), and heteronuclear single quantum correlation (HSQC) spectra confirmed that **5** is the reduction product of **4**. The absolute configuration was assigned as *S* based on the negative and positive Cotton effects in the electronic circular dichroism (ECD) spectrum at 290 and 330 nm (Fig. 5) [24]. Thus, compound **5** was identified as (*S*)-4-(5-(5,7-dihydroxy-4-oxochroman-2-yl)-2-hydroxyphenoxy) benzoic acid and named seladoeflavone N.

Seladoeflavone Q (**6**) was isolated as a yellow amorphous powder with $[\alpha]_D^{20}$ −4.89 (*c* 0.25, MeOH). The molecular formula was determined as $C_{25}H_{20}O_7$ from the pseudomolecular ion peak at *m/z* 431.115 10 $[M - H]^-$ (Calcd. for $C_{25}H_{19}O_7$, 431.113 63) in HR-ESI-MS. NMR data indicated structural similarity to **5** (Table 3). However, HMBCs of H-2' (δ_H 7.28) to C-1'' (δ_C 126.3) and H-6'' (δ_H 7.48) to C-3' (δ_C 125.1) (Fig. 2) indicated a direct C-3'–C-1'' bond between rings B and D. Ring D was confirmed as 1,2,5-trisubstituted benzene by HMBCs of H-4'' (δ_H 7.53)/H-6'' (δ_H 7.48) to C-7'' (δ_C 143.7)/C-2'' (δ_C 157.5) and H-3'' (δ_H 6.90) to C-5'' (δ_C 125.1)/C-1''. Additionally, HMBCs (Fig. 2) of H-7'' (δ_H 7.56), H-8'' (δ_H 6.61) and 9''-Me (δ_H 2.27) to C-9'' (δ_C 197.8), and H-8‴ to C-5‴ (δ_C 125.1) indicated an *α,β*-unsaturated ketone at C-5'' of ring D. The ECD spectrum [24] showed negative and positive Cotton effects at 290 nm and 330 nm, respectively, consistent with the *S* configuration (Fig. 5). Therefore, compound **6** was identified as (*S*, *E*)-2-(2',6-dihydroxy-5'-(3-oxobut-1-en-1-yl)-[1,1'-biphenyl]-3-yl)-5,7-dihydroxychroman-4-one and named seladoeflavone Q.

Compound **7** was isolated as a yellow amorphous powder with $[\alpha]_D^{20}$ −14.22 (*c* 0.25, MeOH). Its molecular formula was determined as $C_{22}H_{16}O_7$ from HR-ESI-MS, which showed a pseudomolecular ion at *m/z* 391.082 70 $[M - H]^-$ (Calcd. for $C_{22}H_{15}O_7$, 391.082 33). NMR data confirmed structural similarity to **6**. HMBCs of H-4'' (δ_H 7.73)/H-6'' (δ_H 7.70) to C-7'' (δ_C 191.2)/C-2'' (δ_C 161.0) and H-3'' (δ_H 7.06) to C-5'' (δ_C 128.1)/C-1'' (δ_C 126.2) indicated a 1,2,5-trisubstituted benzene ring D. Unlike **6**, no signals for a trans double bond or methyl group were observed; instead, an aldehyde signal (1H, s, 5''-CHO) appeared at δ_H 9.82 and δ_C 191.2. HMBCs of H-7'' (δ_H 9.82) to C-5'', H-4''/H-6'' to C-7'', and H-3'' to C-5'' confirmed the aldehyde at C-5''. The ECD spectrum (Fig. 5) showed negative and positive Cotton effects at 290 and 330 nm, indicating the *S* configuration [24]. Thus, compound **7** was identified as (*S*)-5'-(5,7-dihydroxy-4-oxochroman-2-yl)-2',6-dihydroxy-[1,1'-biphenyl]- 3-carbaldehyde.

Compound **8** was isolated as a yellow amorphous powder with $[\alpha]_D^{20}$ −4.00 (*c* 0.25, MeOH). Its molecular formula was determined as $C_{22}H_{16}O_8$ from HR-ESI-MS, which showed a pseudomolecular ion at *m/z* 407.078 30 $[M - H]^-$ (Calcd. for $C_{22}H_{15}O_8$, 407.077 24). 1D and 2D NMR spectra indicated that 8 is a naringenin derivative, similar to **6** and **7**. Ring D was confirmed as 1,2,5-trisubstituted phenyl by HMBCs of H-4''/H-6'' to C-7'' (δ_C 167.4)/C-2'' (δ_C 160.0) and H-3'' to C-5'' (δ_C 120.5)/C-1'' (δ_C

Table 2 ^{1}H NMR (600 MHz) and ^{13}C NMR (150 MHz) data for compounds **4**, **5** and luteolin in DMSO-d_6.

No.	**4**		**5**		Luteolin	
	δ_H	δ_C	δ_H	δ_C	δ_H	δ_C
2	-	162.7	5.48, dd, (12.8, 2.9)	78.0	-	163.9
3	6.88, s	103.8	3.29, dd, (17.1, 12.8) 2.72, dd, (17.1, 2.9)	42.0	6.62, s	102.9
4	-	181.8	-	196.2	-	181.5
5	-	161.4	-	163.5	-	157.3
6	6.19, d, (2.1)	98.9	5.88, d, (2.0)	95.9	6.15, d (1.8)	98.8
7	-	164.3	-	166.8	-	164.0
8	6.49, d, (2.1)	94.1	5.90, d, (2.0)	95.1	6.40, d (1.8)	93.8
9	-	157.3	-	162.8	-	161.5
10	-	103.6	-	101.8	-	103.7
1'	-	122.3	-	130.3	-	119.0
2'	7.88, (overlapped)	121.4	7.25, (overlapped)	121.4	7.38, d (1.8)	113.4
3'	-	141.6	-	141.1	-	145.8
4'	-	153.5	-	149.8	-	149.7
5'	7.16, d (8.5)	117.9	7.04, d, (8.0)	117.4	6.84, d (8.4)	116.0
6'	7.89, (overlapped)	125.3	7.28, (overlapped)	125.1	7.42, dd, (8.4, 1.8)	121.5
1''	-	161.4	-	161.5	-	-
2''	6.94, d (8.9)	115.3	6.90, d (8.9)	115.4	-	-
3''	7.92, d (8.9)	131.5	7.90, d, (8.9)	131.5	-	-
4''	-	124.5	-	124.4	-	-
5''	7.92, d (8.9)	131.5	7.90, d (8.9)	131.5	-	-
6''	6.94, d (8.9)	115.3	6.90, d (8.9)	115.4	-	-
7''	-	166.9	-	166.9	-	-
5-OH	12.91, s	-	12.13, s	-	13.00, s	-

125.6). The key difference from 7 was the presence of a carboxyl group instead of an aldehyde at C-5''. This was confirmed by HMBCs of H-4''/H-6'' to C-7'' and H-3'' to C-5''. Thus, compound **8** was identified as (*S*)-5'-(5,7-dihydroxy-4-oxochroman-2-yl)-2',6-dihydroxy-[1,1'-biphenyl]-3-carboxylic acid.

Comparison of the NMR data (^{1}H, ^{13}C, 2D) of compounds **7** and **8** with those of seladoeflavones C and E from the same plant [19] revealed nearly identical spectroscopic profiles. The main difference was the substitution pattern of ring D: 1,2,5-trisubstituted in **7** and **8** versus 1,3,4-trisubstituted in seladoeflavones C and E. However, HMBCs of the aldehyde proton at δ_H 9.82 to aromatic carbons at δ_C 128.1, 130.5, and 134.0, and of protons at δ_H 7.70 (7.74)/7.73 (7.75) to the aldehyde or carbonyl carbons at δ_C 191.2 (167.4) [19], supported the 1,2,5-trisubstitution pattern. Furthermore, DFT-based ^{13}C NMR calculations (Fig. 4) confirmed that the structures of seladoeflavones C and E should be revised to match those shown in Fig. 1.

Seladoeflavone O (**9**) was isolated as a yellow amorphous powder with $[\alpha]_D^{20}$ +2.67 (*c* 0.25, MeOH). The molecular formula was determined as $C_{31}H_{22}O_{10}$ from the molecular ion peak at *m/z* 555.128 72 $[M + H]^+$ (Calcd. for $C_{31}H_{23}O_{10}$, 555.128 57) in HR-ESI-MS. The ^{1}H NMR spectrum (Table 4) showed two ABX systems: in ring B [δ_H 7.37 (1H, d, *J* = 2.2 Hz, H-2'), 7.34 (1H, dd, *J* = 8.4, 2.2 Hz, H-6'), 6.91 (1H, d, *J* = 8.4 Hz, H-5')] and ring B' [δ_H 7.87 (1H, dd, *J* = 8.6, 2.4 Hz, H-6'''), 7.83 (1H, d, *J* = 2.4 Hz, H-2'''), 6.97 (1H, d, *J* = 8.6 Hz, H-5''')]; two meta-coupled proton pairs in ring A [δ_H 6.13 (1H, d, *J* = 2.3 Hz, H-8), 6.08 (1H, d, *J* = 2.3 Hz, H-6)] and ring A' [δ_H 6.48 (1H, d, *J* = 2.1 Hz, H-8''), 6.18 (1H, d, *J* = 2.1 Hz, H-6'')]; a single aromatic proton at δ_H 6.78 (1H, s, H-3''); and a methoxy signal at δ_H 3.78 (3H s, 7-OMe). An AMX system in the C-ring [δ_H 2.77 (1H, dd, *J* = 17.2, 2.9 Hz, H-3$_{eq}$), 3.42 (1H, dd, *J* = 17.2, 13.0 Hz, H-3$_{ax}$), and 5.55 (1H, dd, *J* = 13.0, 2.9 Hz, H-2)] indicated a dihydroflavonoid. The ^{13}C NMR spectrum showed two conjugated carbonyls at δ_C 197.1 (C-4) and 181.7 (C-4''). These data suggest that **9** is a bis-apigenin-type biflavonoid [7]. DEPT and ^{13}C NMR confirmed 30 carbons from the bis-apigenin skeleton and one methoxy carbon at δ_C 55.9. HMBCs of H-2' to C-3''' and H-2''' to C-3' indicated a C-3'–C-3''' linkage, classifying **9** as a 3',3'''-bis-apigenin. Additionally, HMBCs of H-6/H-8 to C-7 and 7-OMe to C-7 confirmed the methoxy group at C-7. Comparison with 7-*O*-methyl-2,3,2'',3''-tetrahydro-3',3'''-biapigenin [25] revealed structural similarity, except that **9** retains the 2'',3'' double bond. The planar structure was confirmed by HMBC, ^{1}H–^{1}H COSY, and HSQC. The ECD spectrum (Fig. 5) showed a positive Cotton effect at 330 nm and a negative one at 290 nm, indicating an *S* configuration [24]. Thus, compound **9** was identified as (*S*)-2-(2,2'-dihydroxy-5'-(5-hydroxy-7-methoxy-4-oxochroman-2-yl)-[1,1'-biphenyl]-4-yl)-5,7-dihydroxy-4*H*-chromen-4-one and named seladoeflavone O.

Seladoeflavone P (**10**) was isolated as a yellow amorphous powder with $[\alpha]_D^{20}$ +2.22 (*c* 0.24, MeOH). Its molecular formula was determined as $C_{31}H_{22}O_{11}$ from HR-ESI-MS, which showed the $[M + H]^+$ peak at *m/z* 571.123 41 (Calcd. for $C_{31}H_{23}O_{11}$, 571.123 49). NMR data (Table 3) indicated a biflavonoid with two flavonoid units. The key difference from (2*S*)-5'',7''-dihydroxy-2''-phen-

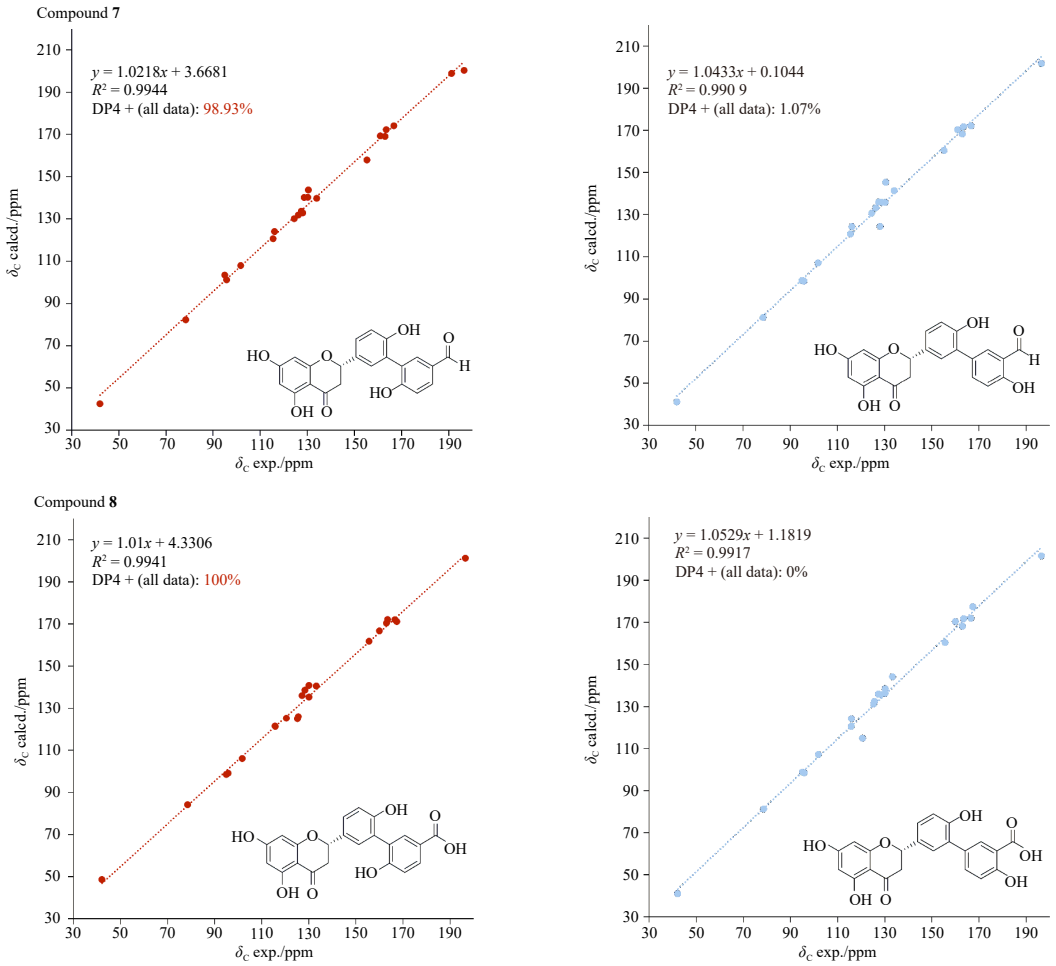

Fig. 4 Linear correlations between the scaled calculated and experimental ^{13}C NMR chemical shifts and statistical DP4 + parameters for compounds **7** and **8**.

oxychromonyl-(4''',3')-naringenin [14] was the presence of a methoxy group at C-7 (δ_C 167.4) instead of a hydroxyl. This was confirmed by HMBCs of 7-OMe (δ_H 3.78, 3H, s) to C-7 and of H-6/H-8 to C-7. The B'-ring was identified as 1,3,4-trisubstituted benzene by HMBCs of H-2'''/H-6''' to C-4''' (δ_C 153.8), H-5''' to C-1''' (δ_C 142.6), and C-3''' (δ_C 126.7). The planar structure was confirmed by HMBC, ^1H–^1H COSY, and HSQC. The ECD spectrum (Fig. 5) showed a positive Cotton effect at 330 nm and a negative one at 290 nm, indicating an *S* configuration [24]. Thus, compound **10** was identified as (*S*)-2-((2',6-dihydroxy-5'-(5-hydroxy-7-methoxy-4-oxochroman-2-yl)-[1,1'-biphenyl]-3-yl)oxy)-5,7-dihy-droxy-4*H*-chromen-4-one and named seladoeflavone P.

The 15 known biflavones were identified as ochnaflavone (**11**) [26], 2,3,2'',3''-tetrahydroochnaflavone (**12**) [27], 2,3-dihydroochnaflavone (**13**) [28], 2'',3''-dihydroochnaflavone (**14**) [29], delicaflavone (**15**) [30], 7-*O*-methyldelicaflavone (**16**) [8], chrysocauloflavone I (**17**) [31], 2,3-dihydro-3',3'''-biapigenin (**18**) [32], involvenflavone G (**19**) [33], 2,3,2'',3''-tetrahydroamentoflavone (**20**) [34], ginkgetin (**21**) [35], putraflavone(**22**) [36], 2,3-dihydrorobustaflavone (**23**) [37], robustaflavone (**24**) [38], and robustaflavone A (**25**) [2], based on comparison of spectroscopic and physicochemical data with literature reports (Fig. 1).

2.2. Initial assessment of anti-cancer properties

S. doederleinii exhibits various pharmacological activities, including anti-microbial, detoxifying, and anti-cancer effects. Among these, its anti-tumor activity has been most extensively documented [39, 40]. The inhibitory effects of 25 compounds were initially evaluated in four representative cancer cell lines: FaDu (hypopharyngeal squamous cell carcinoma), HepG2 (hepatocellular carcinoma), MKN45 (gastric adenocarcinoma), and A549 (lung adenocarcinoma). At 40 μmol·L^{-1}, compounds **12**, **14**, **17**, and **19** exhibited significant inhibition (> 80%) of FaDu cell growth; compounds **12**, **17**, and **19** inhibited HepG2 cell proliferation; and compounds **13** and **17** showed marked activity in MKN45 cells (Fig. 6). None of the compounds showed strong activity against A549 cells. Overall, anti-tumor activity was most pronounced in laryngeal cancer cells. Compounds **12**, **14**, **17**, and **19** are thus potential anti-cancer candidates. However, due to low isolation yields of **12** and **17**, compounds **14** and **19** were selected for further studies in laryngeal cancer cell lines (FaDu and Hep-2).

2.3. Compounds *14* and *19* inhibit the proliferation of the laryngeal cancer cells

The methyl thiazolyl tetrazolium (MTT) assay indicated that compounds **14** and **19** suppressed the proliferation of Hep-2 and FaDu cells in a concentration-dependent manner, with increasing inhibition rates observed at higher concentrations (Figs.7A–7B). The corresponding growth-inhibitory curves and half maximal inhibitory concentration (IC_{50}) values are presented in Fig. 7C. Notably, both compounds exhibited minimal cytotoxicity toward HEK293 cells even at high concentrations, suggesting selective anti-tumor activity (Fig.7C). The IC_{50} values of the positive control cisplatin were 41.89 ± 5.57 μmol·L^{-1} for Hep-2 cells and 47.66 ± 7.17 μmol·L^{-1} for FaDu cells. Upon treatment with compounds **14** and **19**, Hep-2 and FaDu cells displayed prominent plasma membrane blebbing and extensive cellular shrinkage

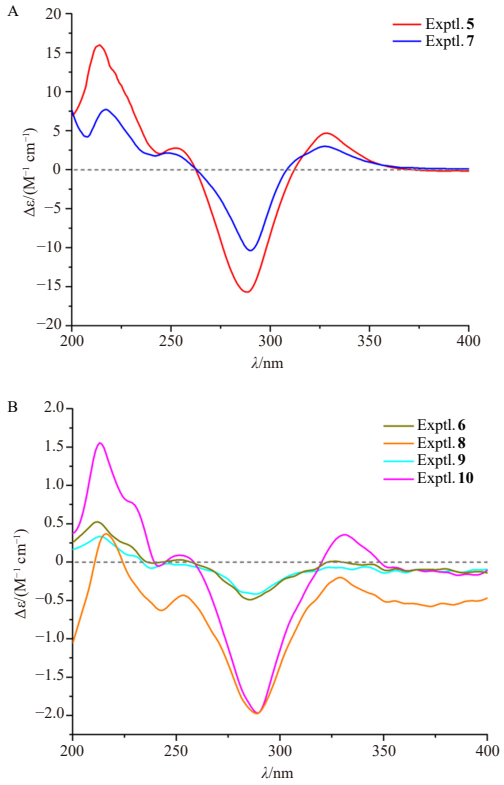

Fig. 5 ECD spectra of compounds **5**–**10**.

(Fig. 7D). These findings demonstrate that compounds **14** and **19** selectively inhibit the growth of laryngeal cancer cells without significant effects on normal cells.

*2.4. Compounds **14** and **19** inhibit the migration of laryngeal cancer cells*

Cell migration was assessed by monitoring the change in scratch area over time. Compared to the control group, compounds **14** and **19** significantly reduced wound healing percentages in Hep-2 and FaDu cells in both dose- and time-dependent manners (Figs. 8A and 8C). Matrix metalloproteinase-9 (MMP-9), a key mediator of cell migration [41], was downregulated by both compounds in Hep-2 and FaDu cells relative to the control (Figs. 8B and 8D). Collectively, these results indicate that compounds **14** and **19** effectively suppress migration in laryngeal cancer cells.

*2.5. Compounds **14** and **19** induce apoptosis in laryngeal cancer cells*

Hoechst 33258 staining revealed an increased number of cells with bright blue apoptotic bodies, positively correlated with the concentration of compounds **14** and **19** in both Hep-2 and FaDu cells (Figs. 9A and 9C). Annexin V-fluorescein isothiocyanate (FITC)/propidium iodide (PI) staining further demonstrated a significant increase in early apoptotic cells (green fluorescence) and late apoptotic cells (red fluorescence) following treatment with **14** and **19** (Figs. 9B and 9D). Together, these data confirm that compounds **14** and **19** promote apoptosis in laryngeal cancer cells.

*2.6. Compounds **14** and **19** induce apoptosis in laryngeal cancer cells via the Akt/mTOR signaling pathway and endoplasmic reticulum (ER) stress, respectively*

We first examined apoptosis-related proteins. Compared to the control, 4 μmol·L^{-1} of compound **14** reduced the Bcl-2/Bax ratio in Hep-2 cells, while 2–4 μmol·L^{-1} of **14** decreased this ratio in FaDu cells. Additionally, 2–4 μmol·L^{-1} of compound **14** upregulated cleaved caspase-3 and cleaved PARP (89 kDa) levels in both Hep-2 and FaDu cells (Fig. 10A). The Akt/mTOR signaling pathway is aberrantly activated in over 90% of head and neck squamous cell carcinomas, including laryngeal cancer [17]. In Hep-2 cells, 2–4 μmol·L^{-1} of compound **14** reduced the expression of p-Akt and p-mTOR (Fig. 10B). In FaDu cells, 2–4 μmol·L^{-1} of **14** downregulated p-Akt, and 4 μmol·L^{-1} reduced p-mTOR levels (Fig. 10B). In both Hep-2 and FaDu cells, 4–8 μmol·L^{-1} of compound **19** significantly reduced the Bcl-2/Bax ratio (Fig. 10C). Cleaved caspase-3 and cleaved PARP levels were elevated by 8 μmol·L^{-1} of **19** in Hep-2 cells and by 4–8 μmol·L^{-1} of **19** in FaDu cells (Fig. 10C). Compound **19** did not alter GRP78 levels in Hep-2 cells, but 4–8 μmol·L^{-1} of **19** reduced GRP78 expression in FaDu cells (Fig. 10D). In Hep-2 cells, 4 μmol·L^{-1} of **19** increased cleaved caspase-12, and 8 μmol·L^{-1} elevated cleaved caspase-7 (Fig. 10D). In FaDu cells, 4–8 μmol·L^{-1} **19** upregulated cleaved caspase-12, and 8 μmol·L^{-1} increased cleaved caspase-7 (Fig. 10D). Inhibiting the Akt/mTOR pathway or the adaptive arm of ER stress signaling has been shown to overcome drug resistance and improve prognosis in tumors. Taken together, these findings indicate that compound **14** induces apoptosis partially through the Akt/mTOR pathway, whereas compound **19** acts *via* ER stress pathways.

3. Conclusions

In the petroleum ether and ethyl acetate fractions of the whole herbs of *S. doederleinii*, ten new flavonoids, seladoeflavones J–Q, C, and E (**1**–**10**), were isolated, along with fifteen known biflavones. Compounds **14** and **19** exhibited the most potent activity in inhibiting the proliferation of laryngeal cancer cells (Hep-2 and FaDu) and inducing apoptosis. Compound **14** triggered apoptosis by suppressing the Akt/mTOR signaling pathway, whereas compound **19** downregulated ER stress pathways. This study identifies the major bioactive constituents of *S. doederleinii* and proposes their potential molecular mechanisms, thereby expanding the structural diversity and anti-laryngeal cancer activities associated with this plant. In future work, compounds **14** and **19** will be prepared in larger quantities to enable in-depth investigation of their anti-laryngeal cancer mechanisms.

4. Experimental

4.1. General experimental procedures

The detailed information has been provided in the Supplementary Material.

4.2. Plant material

The whole dried plants of *S. doederleinii* were collected from Nanning, Guangxi Zhuang Autonomous Region, China, in July 2019. The plant material was authenticated by Prof. Dingrong Wan, an expert at South-Central Minzu University (SCMU). A voucher specimen (No. SC0611) is deposited in the School of Pharmaceutical Sciences, SCMU, Wuhan, China.

4.3. Extraction and isolation

Air-dried *S. doederleinii* (whole herbs, 40.0 kg) were ground and exhaustively extracted four times with 80% EtOH (50 L, 3 days per extraction). The resulting extract was suspended in warm water and sequentially partitioned with petroleum ether, ethyl acetate, and *n*-butanol. The combined petroleum ether

Table 3 ^{1}H NMR (600 MHz) and ^{13}C NMR (150 MHz) data for compounds **6**–**10** in DMSO-d_6.

No.	**6**		**7**		**8**		**9**		**10**	
	δ_H	δ_C	δ_H	δ_C	δ_H	δ_C	δ_H	δ_C	δ_H	δ_C
2	5.47, dd (13.0, 2.9)	78.6	5.48, dd (13.0, 2.8)	78.5	5.47, dd (13.0, 2.9)	78.6	5.55, dd (13.0, 2.9)	78.8	5.52, dd (13.1, 2.8)	78.7
3	3.31 (overlapped) 2.69, dd (17.1, 2.9)	42.1	3.31 (overlapped) 2.69, dd (17.1, 2.8)	42.0	3.31 (overlapped) 2.69, dd (17.2, 2.9)	42.1	3.42, dd (17.2, 13.0) 2.77, dd (17.2, 2.9)	42.1	3.37 (overlapped) 2.73, dd, (17.1, 2.8)	42.1
4	-	196.5	-	196.5	-	196.5	-	197.2	-	197.0
5	-	163.5	-	163.5	-	163.5	-	163.2	-	163.2
6	5.88, d (2.1)	95.8	5.88, d (2.1)	95.8	5.89, d (1.9)	95.8	6.08, d (2.3)	94.7	6.07, d (2.3)	94.7
7	-	166.7	-	166.7	-	166.6	-	167.4	-	167.4
8	5.89, d (2.1)	95.0	5.89, d (2.1)	95.0	5.89, d (1.9)	95.0	6.13, d (2.3)	93.8	6.11, d (2.3)	93.8
9	-	163.0	-	163.0	-	163.0	-	163.0	-	162.9
10	-	101.8	-	101.8	-	101.8	-	102.6	-	102.6
1'	-	128.6	-	128.7	-	128.4	-	128.2	-	128.3
2'	7.28, d (2.3)	130.3	7.30, d (2.3)	130.2	7.28, d (2.2)	130.1	7.37, d (2.2)	130.1	7.36, d (2.2)	130.3
3'	-	125.1	-	124.5	-	125.2	-	125.4	-	124.5
4'	-	155.3	-	155.3	-	155.6	-	156.3	-	155.4
5'	6.92, (overlapped)	115.5	6.94 d (8.3)	115.5	6.90, (overlapped)	115.7	6.91, d (8.4)	116.0	6.93, d (8.3)	115.8
6'	7.31, dd (8.4, 2.3)	127.3	7.34, dd (8.3, 2.3)	127.5	7.31, dd (8.4, 2.2)	127.2	7.34, dd (8.4, 2.2)	127.2	7.33, dd (8.3, 2.2)	127.4
1''	-	126.3	-	126.2	-	125.6				
2''	-	157.5	-	161.0	-	160.0	-	164.2	-	168.1
3''	6.90, (overlapped)	116.2	7.06, d (8.4)	116.1	6.91 (overlapped)	115.8	6.78, s	102.6	5.15, s	86.9
4''	7.53, dd (8.5, 2.2)	128.9	7.73, dd (8.4, 2.2)	130.5	7.75 (overlapped)	133.2	-	181.7	-	183.1
5''	-	125.1	-	128.1	-	120.5	-	161.5	-	161.4
6''	7.48, d (2.2)	132.4	7.70, d (2.2)	134.0	7.74 (overlapped)	130.1	6.18, d (2.1)	98.8	6.19, d (2.0)	99.2
7''	7.56, d (16.3)	143.7	9.82	191.2	-	167.4	-	164.1	-	163.9
8''	6.61, d (16.3)	124.1	-	-	-	-	6.48, d (2.1)	94.0	6.37, d (2.0)	93.9
9''	-	197.8	-	-	-	-	-	157.3	-	154.8
10''	-	-	-	-	-	-	-	103.7	-	101.9
1'''	-	-	-	-	-	-	-	119.8	-	142.6
2'''	-	-	-	-	-	-	7.83, dd (2.4)	129.7	7.17, d (1.9)	123.5
3'''	-	-	-	-	-	-	-	127.0	-	126.7
4'''	-	-	-	-	-	-	-	161.0	-	153.8
5'''	-	-	-	-	-	-	6.97, d (8.6)	116.9	6.98, d (9.2)	116.8
6'''	-	-	-	-	-	-	7.89, dd (8.6, 2.4)	127.2	7.16, (overlapped)	120.4
7-OMe	-	-	-	-	-	-	3.78, s	55.9	3.78, s	55.9
9''-Me	2.27, s	27.23	-	-	-	-				
5-OH	12.16, s	-	12.16, s	-	12.16, s	-	12.14, s	-	12.12, s	-
5''-OH	-	-	-	-	-	-	13.04, s	-	12.82, s	-

(345.0 g) and ethyl acetate (501.0 g) fractions were subjected to HP-20 macroporous resin column chromatography (CC). Gradient elution was performed using EtOH in H_2O (10%→20%→30%→40%→50%→60%→70%→80%→95%→anhydrous ethanol), followed by anhydrous ethanol: ethyl acetate (1∶1). The eluates were pooled into nine fractions (Fr. A–Fr. I) based on TLC

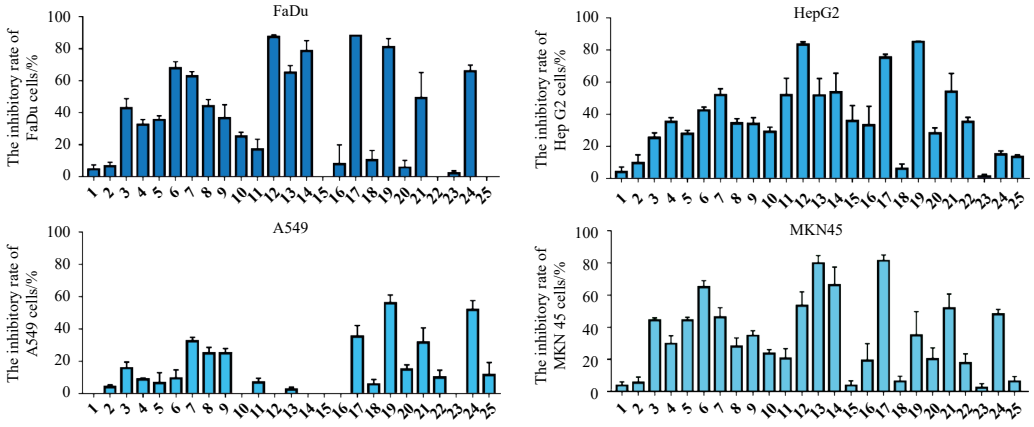

Fig. 6 Inhibitory effects of compounds **1–25** (40 μmol·L^{-1}) on the viability of FaDu, HepG2, A549, and MKN45 cells (Means ± SD, n = 3). The inhibition rate was determined by comparing to the untreated cells (0 μmol·L^{-1}).

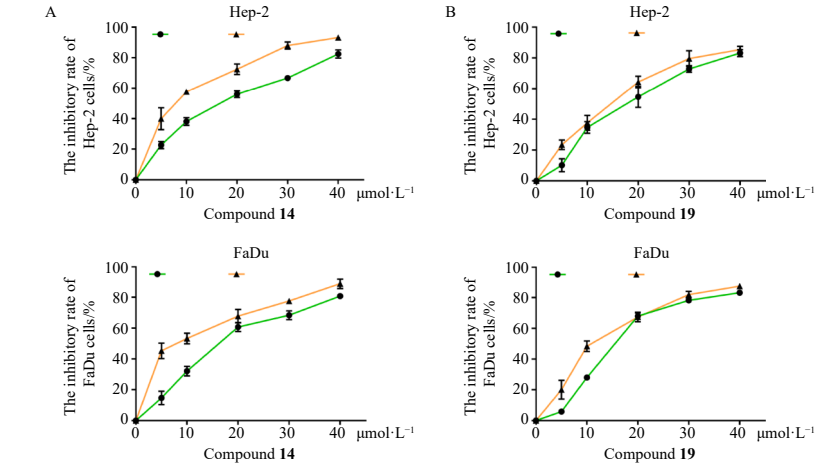

C

Cytotoxic activity of compound **14** against throat carcinoma and embryonic kidney cells (Mean ± SD, n = 3)

t/h	IC_{50}/(μmol·L^{-1})		
	Hep-2	FaDu	HEK293
12	14.97 ± 0.48	16.11 ± 1.22	> 100
24	7.37 ± 0.98	7.22 ± 0.80	> 100

Cytotoxic activity of compound **19** against throat carcinoma and embryonic kidney cells (Mean ± SD, n = 3)

t/h	IC_{50}/(μmol·L^{-1})		
	Hep-2	FaDu	HEK293
12	16.97 ± 1.61	15.45 ± 0.41	> 100
24	12.86 ± 0.60	11.37 ± 0.29	> 100

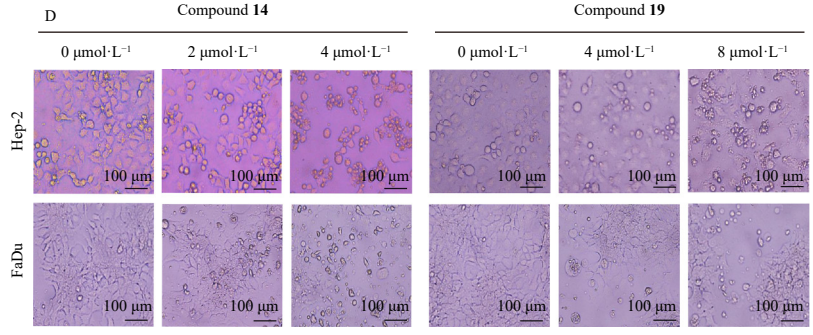

Fig. 7 The effects of compounds **14** and **19** on cell viability and morphology in laryngeal cancer cells. (A–B) Cell inhibition rate (0, 5, 10, 20, 30, 40 μmol·L^{-1}). (C) The IC_{50} of Hep-2, FaDu, and HEK293 cells. (D) Morphological images of Hep-2 and FaDu cells treated with compounds **14** (0, 2, 4 μmol·L^{-1}) or **19** (0, 4, 8 μmol·L^{-1}) for 24 h (magnification 200 ×). The inhibition rate was determined by comparing to the untreated cells (0 μmol·L^{-1}), Means ± SD (n = 3).

analysis.

Fr. E was separated on a silica gel CC using a $CHCl_3$–MeOH gradient (100∶1 to 1∶100, *V/V*), yielding six fractions (Fr. E1–Fr. E6). Fr. E2 was further fractionated by Sephadex LH-20 CC with MeOH elution to afford three subfractions (Fr. E2-1–Fr. E2-3). Fr. E2-3 was purified by semi-preparative high-performance liquid chromatography (HPLC) ($CNCH_3/H_2O$, 40∶60–65∶35, *V/V*, 40 min, 0.1% formic acid in both phases) to yield compound **2** (3.0 mg). Fr. E3 was chromatographed on Sephadex LH-20 CC with MeOH elution to give three subfractions (Fr. E3-1–Fr. E3-3). Fr. E3-3 was purified by semi-preparative HPLC ($CNCH_3/H_2O$, 35∶65→75∶25, *V/V*, 40 min, 0.1% formic acid) to afford compounds **6** (6.9 mg) and **7** (10.0 mg). Fr. E4 was fractionated by Sephadex LH-20 CC with MeOH elution into six subfractions (Fr.

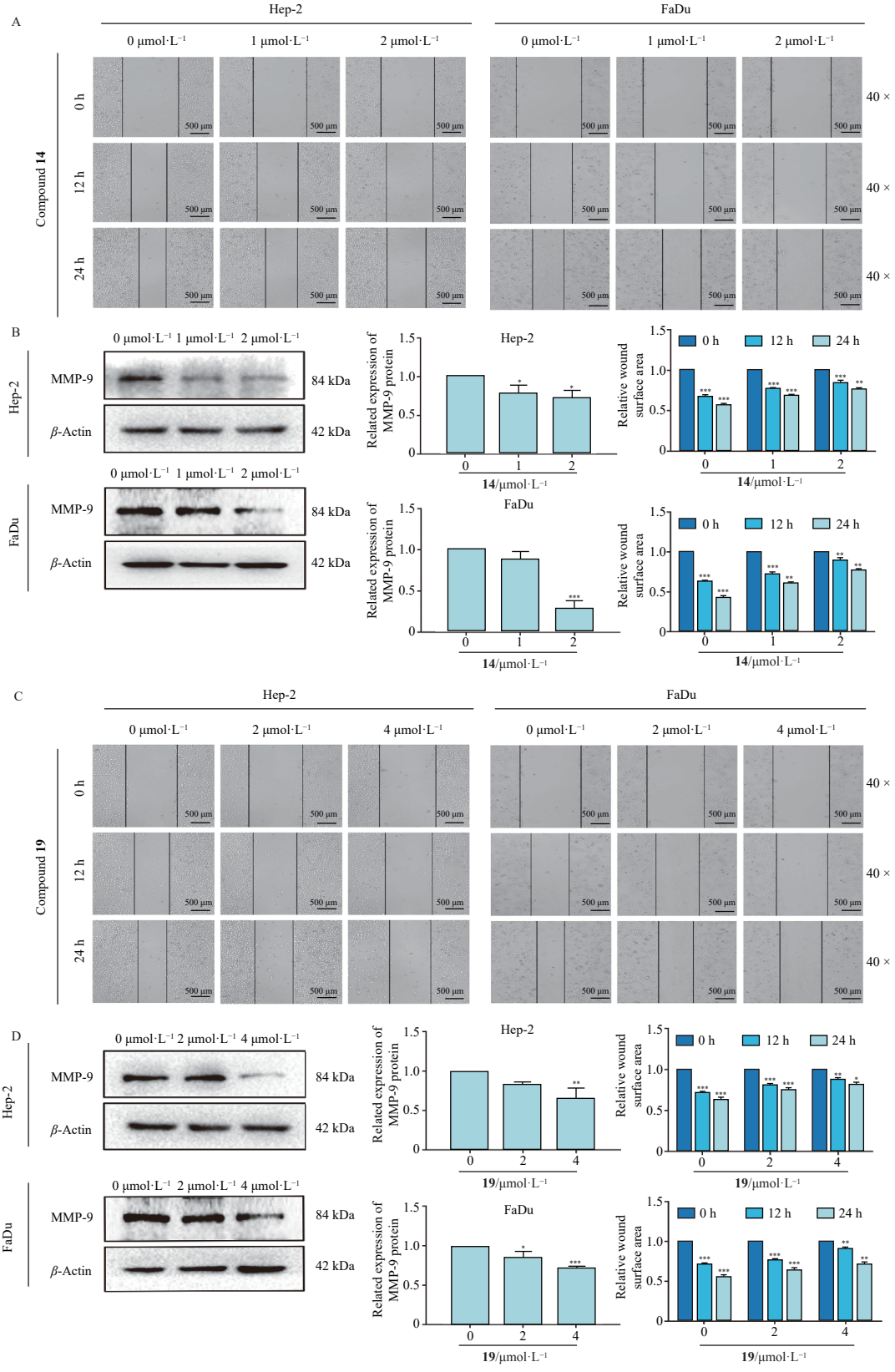

Fig. 8 Compounds **14** and **19** inhibit the migration of laryngeal cancer cells. (A) Scratch assay of Hep-2 and FaDu cells treated with compound **14** (magnification 40 ×). (B) The MMP-9 expression in Hep-2 and FaDu cells treated with compound **14**. (C) Scratch assay with compound **19** (magnification 40 ×). (D) The MMP-9 expression with compound **19**. Means ± SD (n = 3). $^{*}P < 0.05$, $^{**}P < 0.01$, $^{***}P < 0.001$ *vs* control (0 μmol·L^{-1}).

E4-1–Fr. E4-6). Fr. E4-4 was purified by semi-preparative HPLC ($CNCH_3/H_2O$, 35∶65→75∶25, *V/V*, 40 min, 0.1% formic acid) to yield two components (Fr. E4-4-1 and Fr. E4-4-2). Fr. E4-4-1 was further purified by semi-preparative HPLC ($CNCH_3/H_2O$, 40∶60→50∶50, *V/V*, 35 min, 0.1% formic acid) to obtain compounds **1** (8.7 mg) and **8** (22.5 mg). Compound **5** (3.8 mg) was isolated from Fr. E4-4-2 by repeated semi-preparative HPLC ($CNCH_3/H_2O$, 40∶60→50∶50, *V/V*, 35 min, 0.1% formic acid). Fr. E4-5 was purified by semi-preparative HPLC ($CNCH_3/H_2O$, 10∶90→90∶10, *V/V*, 110 min, 0.1 % formic acid) to yield com-

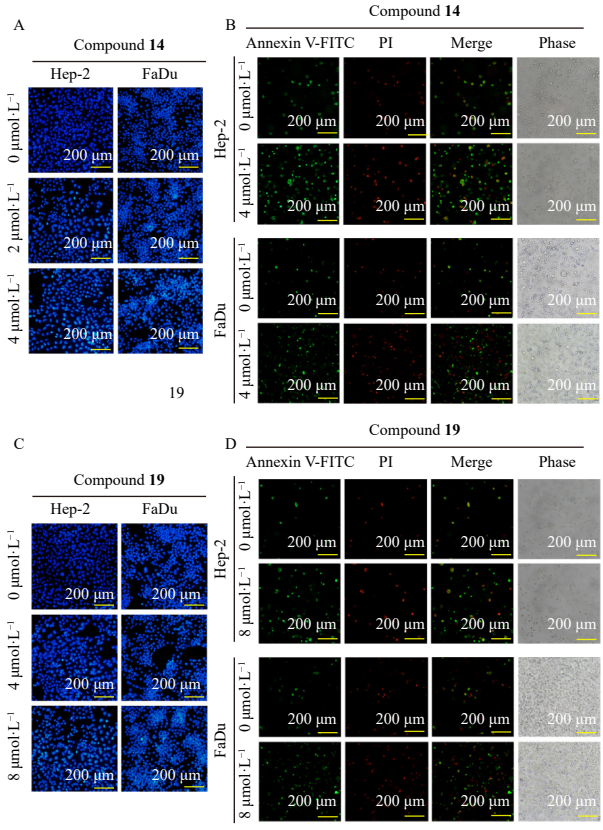

Fig. 9 Compounds **14** and **19** induce apoptosis in laryngeal cancer cells. (A–B) Hoechst 33258 staining and Annexin V-FITC and PI staining of two laryngeal cancer cells treated with compound **14** (0, 2, 4 μmol·L^{-1}) for 24 h. (C–D) Two types of staining of cells treated with compound **19** (0, 4, 8 μmol·L^{-1}) for 24 h. (magnification 100 ×).

pounds **3** (4.9 mg) and **4** (3.1 mg). Fr. E4-6 was purified by semi-preparative HPLC to obtain **18** (5.1 mg), **20** (4.3 mg), **23** (3.6 mg), and **24** (2.3 mg) Fr. F was separated on a silica gel CC with $CHCl_3$–MeOH elution (100∶1 to 1∶100, *V/V*) into eight fractions (Fr. F1–Fr. F8). Fr. F7 was purified by semi-preparative HPLC ($CNCH_3/H_2O$, 35∶65→90∶10, *V/V*, 40 min, 0.1% formic acid) to yield compounds **11** (4.6 mg) and **15** (36.7 mg). Fr. G was separated on a silica gel CC with $CHCl_3$–MeOH gradient elution (100∶1 to 1∶100, *V/V*) into five fractions (Fr. G1–Fr. G5). Fr. G4 was further fractionated by Sephadex LH-20 CC with MeOH elution into three subfractions (Fr. G4-1–Fr. G4-3). Fr. G4-3 was purified by semi-preparative HPLC ($CNCH_3/H_2O$, 40∶60→10∶90, *V/V*, 50 min, 0.1% formic acid) to yield seven subfractions (Fr. G4-3-1–Fr. G4-3-7). Fr. G4-3-5 was purified to afford compounds **12** (20.1 mg), **13** (20.3 mg), **14** (196.5 mg), and **17** (30.7 mg). Fr. G4-3-6 was purified to yield compounds **9** (2.8 mg), **10** (3.1 mg), **19** (86.8 mg), **21** (5.0 mg), and **22** (13.9 mg). Compounds **16** (71.7 mg) and **25** (10.0 mg) were isolated from Fr. G4-3-7 by repeated semi-preparative HPLC.

*4.4. Spectroscopic data of compounds **1–10***

Seladoeflavone J (**1**): Yellow powder; UV λ_{max} (MeOH, nm) (log ε) 221 (2.84), 265 (3.49) and 345 (2.29); IR ν_{max} (cm^{-1}): 3240, 1651, 1600, 1504 and 1442; ^{1}H and ^{13}C NMR spectroscopic data are given in Table 1; HR-ESI-MS *m/z* 407.076 02 [M + H]$^+$ (Calcd. for $C_{22}H_{15}O_8$: 407.076 14).

Seladoeflavone K (**2**): Yellow powder; UV λ_{max} (MeOH, nm) (log ε) 221 (2.98), 270 (3.48) and 346 (2.04); IR ν_{max} (cm^{-1}): 3309, 1654, 1608, 1597, 1554; ^{1}H and ^{13}C NMR spectroscopic data are given in Table 1; HR-ESI-MS *m/z* 427.078 92 [M + Na]$^+$ (Calcd. for $C_{23}H_{16}O_7Na$: 427.078 82).

Seladoeflavone L (**3**): Yellow powder; UV λ_{max} (MeOH, nm) (log ε) 238 (3.85) and 320 (5.01); IR ν_{max} (cm^{-1}): 3367, 1651, 1500, 1423; ^{1}H and ^{13}C NMR spectroscopic data are given in Table 1; HR-ESI-MS *m/z* 407.075 99 [M + H]$^+$ (Calcd. for $C_{22}H_{15}O_8$: 407.076 14).

Seladoeflavone M (**4**): Yellow powder; UV λ_{max} (MeOH, nm) (log ε) 234 (3.85) and 320 (5.01); IR ν_{max} (cm^{-1}): 3302, 1658, 1597 and 1508; ^{1}H and ^{13}C NMR spectroscopic data are given in Table 2; HR-ESI MS *m/z* 407.075 99 [M + H]$^+$ (Calcd. for $C_{22}H_{15}O_8$: 407.076 14).

Seladoeflavone N (**5**): Yellow powder; $[\alpha]_D^{20}$ −3.97 (*c* 0.42, MeOH); UV λ_{max} (MeOH, nm) (log ε) 235 (3.76) and 308 (3.56); IR ν_{max} (cm^{-1}): 3155, 1701, 1604, 1516 and 1465; ECD (*c* 0.42, MeOH) $\lambda_{max}(\Delta\varepsilon)$ 290 (−10.36) nm, 328 (3.07) nm; ^{1}H and ^{13}C NMR spectroscopic data are given in Table 2; HR-ESI-MS *m/z* 409.091 74 [M + H]$^+$ (Calcd. for $C_{22}H_{17}O_8$: 409.091 79).

Seladoeflavone Q (**6**): Yellow powder; $[\alpha]_D^{20}$ −4.89 (*c* 0.25, MeOH); UV λ_{max} (MeOH, nm) (log ε) 210 (1.80), 291 (1.08); IR ν_{max} (cm^{-1}): 3367, 1651, 1450, 1415; ^{1}H and ^{13}C NMR spectroscopic data are given in Table 3; HR-ESI-MS *m/z* 431.115 10 [M − H]$^-$ (Calcd. for $C_{25}H_{19}O_7$: 431.113 63).

Seladoeflavone C (**7**): Yellow powder; $[\alpha]_D^{20}$ −14.22 (*c* 0.25, MeOH); UV λ_{max} (MeOH, nm) (log ε) 215 (2.18), 290 (1.31); IR ν_{max} (cm^{-1}): 3410, 1643, 1483; ^{1}H and ^{13}C NMR spectroscopic data are given in Table 3; HR-ESI-MS *m/z* 391.082 70 [M − H]$^-$ (Calcd. for $C_{22}H_{15}O_7$: 391.082 33).

Seladoeflavone E (**8**): Yellow powder; $[\alpha]_D^{20}$ −4.00 (c 0.25, MeOH); UV λ_{max} (MeOH, nm) (log ε) 215 (1.69), 287 (0.77); IR ν_{max} (cm^{-1}): 3375, 1654, 1450, 1411; ^{1}H and ^{13}C NMR spectroscopic data are given in Table 3; HR-ESI-MS *m/z* 407.078 30 [M − H]$^-$ (Calcd. for $C_{22}H_{15}O_8$: 407.077 24).

Seladoeflavone O (**9**): Yellow powder; $[\alpha]_D^{20}$ +2.67 (*c* 0.25, MeOH); UV λ_{max} (MeOH, nm) (log ε) 215 (2.66), 289 (1.52), 335 (1.13); IR ν_{max} (cm^{-1}): 3414, 1647, 1504, 1469; ECD (c 0.25, MeOH) $\lambda_{max}(\Delta\varepsilon)$ 290 (−0.36) nm, 328 (−0.11) nm; ^{1}H and ^{13}C NMR spectroscopic data are given in Table 3; HR-ESI-MS *m/z* 555.128 72 [M + H]$^+$ (Calcd. for $C_{31}H_{23}O_{10}$: 555.128 57).

Seladoeflavone P (**10**): Yellow powder; $[\alpha]_D^{20}$ +2.22 (*c* 0.24, MeOH); UV λ_{max} (MeOH, nm) (log ε) 235 (3.76), 290 (3.40); IR ν_{max} (cm^{-1}): 3398, 1643, 1419; ECD (*c* 0.24, MeOH) $\lambda_{max}(\Delta\varepsilon)$ 290 (−1.92) nm, 330 (0.35) nm; ^{1}H and ^{13}C NMR spectroscopic data are given in Table 3; HR-ESI-MS *m/z* 571.123 41 [M + H]$^+$ (Calcd. for $C_{31}H_{23}O_{11}$: 571.123 49).

4.5. NMR calculation

The conformations of compounds **1**–**5**, **7**, and **8** were determined by a random conformational search in Sybyl-X 2.1.1 using the MMFF94S force field. The resulting stable conformers were optimized using Gaussian 09 at the B3LYP/6-31G(d) level. GIAO shielding constants were calculated at the mPW1PW91/6-311 + G(d, p) level with the PCM model. The calculated ^{1}H and ^{13}C NMR chemical shifts were averaged according to Boltzmann distribution theory, using relative Gibbs free energies with TMS as reference. Experimental and calculated NMR data were analyzed using the DP4 + method in an Excel sheet provided by Grimblat et al [42,43].

4.6. Cell culture

HEK293 (embryonic kidney), FaDu, Hep-2, HepG2, MKN45, and A549 cells were obtained from the Shanghai Institute of Biochemistry and Cell Biology. Except for FaDu cells, which were cultured in MEM medium, all other cells were maintained in DMEM supplemented with 10% FBS. Cells were grown to approximately 80% confluence before treatment with compounds **1**–**25**. Cisplatin was used as the positive control.

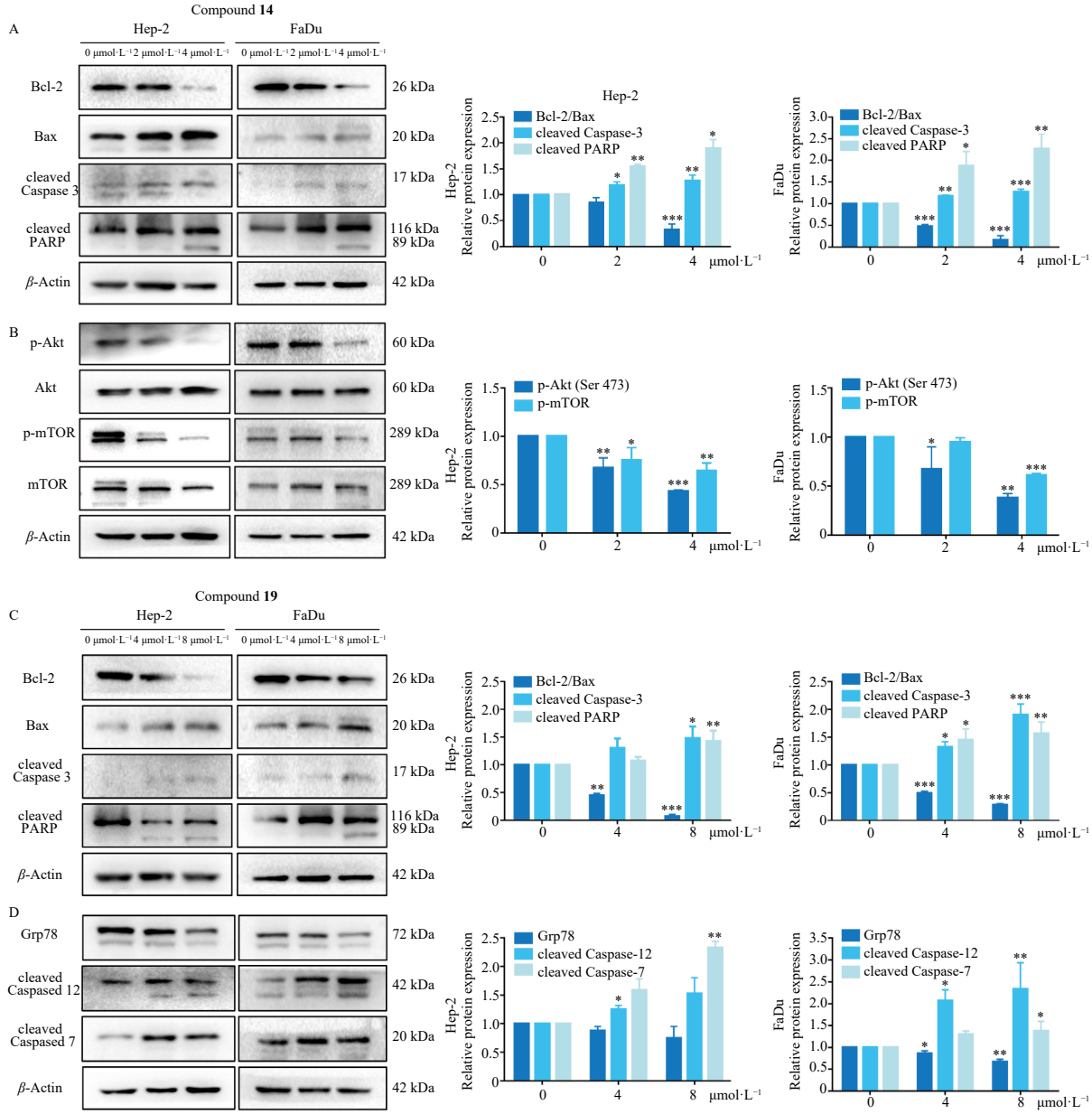

Fig. 10 Compounds **14** and **19** promote apoptosis in laryngeal cancer cells *via* the Akt/mTOR signaling pathway and endoplasmic reticulum (ER) stress, respectively. Cells were incubated with compound **14** (0, 2, 4 μmol·L^{-1}) or compound **19** (0, 4, 8 μmol·L^{-1}). Means ± SD (n = 3). $^{*}P < 0.05$, $^{**}P < 0.01$, $^{***}P < 0.001$ *vs* control (0 μmol·L^{-1}).

4.7. Cell viability assay

Cells were given compounds **1**–**25** (40 μmol·L^{-1}) for 24 h. Then, MTT was used to evaluate cell viability. The absorbance was measured at 562 nm. The inhibitory rate was calculated by $\left(1-\frac{A_{sample}-A_{blank}}{A_{control}-A_{blank}}\right)\times 100\%$.

4.8. Morphology observation and Hoechst 33258 staining

Hep-2 and FaDu cells were treated with compound **14** (0, 2, 4 μmol·L^{-1}) or compound **19** (0, 4, 8 μmol·L^{-1}) for 24 h. Morphological changes were recorded (magnification 100 ×). Apoptotic cells were detected by Hoechst 33258 staining, and fluorescence images were captured (magnification 100 ×).

4.9. Wound healing assay

Hep-2 and FaDu cells were treated with compound **14** (0, 1, 2 μmol·L^{-1}) or compound **19** (0, 2, 4 μmol·L^{-1}). A wound was created by scraping the cell monolayer. Images were captured at 0, 12, and 24 h (magnification 40 ×). Wound closure was quantified using ImageJ software.

4.10. Annexin V-FITC/PI staining assay

Cells were incubated with compound **14** (0, 2, 4 μmol·L^{-1}) or compound **19** (0, 4, 8 μmol·L^{-1}) for 24 h. After trypsinization, cells were stained with Annexin V-FITC and PI. Fluorescence images were acquired (magnification 100 ×).

4.11. Western blots

Cellular proteins were extracted using RIPA lysis buffer. Proteins were separated by SDS-PAGE and transferred to PVDF membranes. Membranes were blocked with 5% skim milk, incubated with primary antibody at 4 °C overnight, and then with secondary antibody for 1 h. Protein bands were visualized using the HRP-ECL detection system.

4.12. Statistical analysis

All data were expressed as means ± SD. One-way analysis of variance (ANOVA) and Tukey's post hoc test were used for comparisons between multiple groups. Statistical significance is defined as a P value < 0.05.

Funding

The work was supported by the National Natural Science Foundation of China (No. 81774000), State Key Laboratory of Drug Research (No. SKLDR-2024-KF-05), the Fundamental Research Funds for the Central Universities, South-Central MinZu University (Nos. CZD24003 and XTZ24026), and Tianchi Talent-Distinguished Professor Program.

Declaration of competing interest

The authors declare that they have no known competingfinancial interests or personal relationships that could haveappeared to influence the work reported in this paper.

References

1 Sung H, Ferlay J, Siegel RL, et al. Global cancer statistics 2020: GLOBOCAN estimates of incidence and mortality worldwide for 36 cancers in 185 countries. *Ca-Cancer J Clin*. 2021;71(3):209-249. https://doi.org/10.3322/caac.21660.
2 Xie Y, Zhou X, Li J, et al. Identification of a new natural biflavonoids against breast cancer cells induced ferroptosis *via* the mitochondrial pathway. *Bioorg Chem*. 2021;109:104744. https://doi.org/10.1016/j.bioorg.2021.104744.
3 Qin SS, Pan ZL, Wang C, et al. Effects of paclitaxel on immune cells in tumor therapy. *J Yichun Univ*. 2022;44:26-28. https://doi.org/10.3969/j.issn.1671-380X.2022.12.006.
4 Zhao TT, Cai ZD, Du LL, et al. Research on delivery systems of camptothecin-based antitumour drugs. *J New Drugs*. 2023;32:246-254. https://doi.org/10.3969/j.issn.1003-3734.2023.03.006.
5 Guerram M, Jiang ZZ, Zhang LY. Podophyllotoxin, a medicinal agent of plant origin: past, present and future. *Chin J Nat Med*. 2012;10(3):161-169. https://doi.org/10.3724/SP.J.1009.2012.00161.
6 Xu ZC, Fu XX, Jin LL. Chemical constituents research progress of *Selaginella tamariscina*. *Chin J Mod Appl Pharm*. 2017;34:1779-1784. https://doi.org/10.13748/j.cnki.issn1007-7693.2017.12.030.
7 Xie Y, Xu KP, Zou ZX, et al. Advances in chemodiversity from *Selaginella*. *Cent South Pharm*. 2017;15:129-142. https://doi.org/10.7539/j.issn.1672-2981.2017.02.001.
8 Kang FH, Zhang S, Chen DK, et al. Biflavonoids from *Selaginella doederleinii* as potential antitumor agents for intervention of non-small cell lung cancer. *Molecules*. 2021;26(17):5401. https://doi.org/10.3390/molecules26175401.
9 Li SG, Li ZJ, Li H, et al. Synthesis, biological evaluation, pharmacokinetic studies and molecular docking of 4"-acetyl-delicaflavone as antitumor agents. *Bioorg Chem*. 2022;120:105638. https://doi.org/10.1016/j.bioorg.2022.105638.
10 Xu DF, Wang XW, Huang DD, et al. Disclosing targets and pharmacological mechanisms of total bioflavonoids extracted from *Selaginella doederleinii* against non-small cell lung cancer by combination of network pharmacology and proteomics. *J Ethnopharmacol*. 2022;286:114836. https://doi.org/10.1016/j.jep.2021.114836.
11 Wang SS, Wan DR, Liu WQ, et al. A biflavonoid-rich extract from *Selaginella doederleinii* Hieron. against throat carcinoma *via* Akt/Bad and IKKβ/NF-κB/COX-2 pathways. *Pharmaceuticals-Base*. 2022;15(12):1505. https://doi.org/10.3390/ph15121505.
12 Wang G, Zhang MS, Li D, et al. Study on chemical constituents of *Selaginella doederleinii*. *Liaoning J Tradit Chin Med*. 2019;46:124-126. https://doi.org/10.13192/j.issn.1000-1719.2019.01.041.
13 Jin XD, Lu X, Wang HG, et al. Advances in research on chemical constituents and pharmacological activities of Genus *Selaginella*. *Lishizhen Med Mater Med Res*. 2018;29:959-963. https://doi.org/10.3969/j.issn.1008-0805.2018.04.069.
14 Liu LF, Sun HH, Tan JB, et al. New cytotoxic biflavones from *Selaginell adoederleinii*. *Nat Prod Res*. 2019;35(6):930-936. https://doi.org/10.1080/14786419.2019.1611813.
15 Chen M, Zheng N, Liu W, et al. Seladoeneolignan A, a new neolignan from *Selaginella doederleinii* Hieron. *J Holistic Integr Pharm*. 2022;3(3):224-229. https://doi.org/10.1016/S2707-3688(23)00042-0.
16 Kim C, Kim B. Anti-cancer natural products and their bioactive compounds inducing ER stress-mediated apoptosis: a review. *Nutrients*. 2018;10(8):1021. https://doi.org/10.3390/nu10081021.
17 Marquard FE, Jücker M. PI3K/AKT/mTOR signaling as a molecular target in head and neck cancer. *Biochem Pharmacol*. 2020;172:113729. https://doi.org/10.1016/j.bcp.2019.113729.
18 Zou ZX, Xu PS, Zhang GG, et al. Selagintriflavonoids with BACE1 inhibitory activity from the fern *Selaginella doederleinii*. *Phytochemistry*. 2017;134:114-121. https://doi.org/10.1016/j.phytochem.2016.11.011.
19 Zou Z, Xu K, Xu P, et al. Seladoeflavones A–F, six novel flavonoids from *Selaginella doederleinii*. *Fitoterapia*. 2017;116:66-71. https://doi.org/10.1016/j.fitote.2016.11.014.
20 Jia MY, Li XZ, Jia XY, et al. Chemical constituents from the aerial parts of *Caragana turfanensis*. *Chin Tradit Pat Med*. 2021;43(9):2388-2392. https://doi.org/10.3969/j.issn.1001-1528.2021.09.020.
21 Chen MA, Lin CH, Liang X. Chemical constituents from the ethyl acetate fraction of *Caryopteris incana*. *Chin Tradit Pat Med*. 2021;43:939-943. https://doi.org/10.3969/j.issn.1001-1528.2021.04.020.
22 Chen MY, Wang SS, Cheng HT, et al. Seladoeflavones G–I, three new flavonoids from *Selaginella doederleinii* Hieron. *Chem Select*. 2022;7(37):e202202242. https://doi.org/10.1002/slct.202202242.
23 Jia RF, Liu HX, Huang ML, et al. Chemical constituents from *Agastache rugosa*. *Chin Tradit Herb Drugs*. 2021;52(10):2884-2889. https://doi.org/10.7501/j.issn.0253-2670.2021.10.004.
24 Slade D, Ferreira D, Marais JP. Circular dichroism, a powerful tool for the assessment of absolute configuration of flavonoids. *Phytochemistry*. 2005;66(18):2177-2215. https://doi.org/10.1016/j.phytochem.2005.02.002.
25 Zou ZX, Zhang S, Tan JB, et al. Two new biflavonoids from *Selaginella doederleinii*. *Phytochem Lett*. 2020;40:126-129. https://doi.org/10.1016/j.phytol.2020.10.003.
26 Jia XH, Tang WZ, Yan HJ, et al. A new organic acid from Lonicerae Japonicae Caulis produced in Shandong. *Chin Tradit Herb Drugs*. 2016;47:3766-3768. https://doi.org/10.7501/j.issn.0253-2670.2016.21.002.
27 Ariyasena J, Baek SH, Perry NB, et al. Ether-linked biflavonoids from *Quintinia acutifolia*. *J Nat Prod*. 2004;67(4):693-696. https://doi.org/10.1021/np0340394.
28 Rao KV, Sreeramulu K, Rao CV, et al. Two new biflavonoids from *Ochna obtusata*. *J Nat Prod*. 1997;60(6):632-634. https://doi.org/10.1021/np9604590.
29 de Oliveira MCC, de Carvalho MG, da Silva CJ, et al. New biflavonoid and other constituents from *Luxemburgia nobilis* (ElCHL). *J Brazil Chem Soc*. 2002;13(1):119-123. https://doi.org/10.1590/S0103-50532002000100020.
30 Long HP, Li FS, Xu KP, et al. Chemical constituents from *Selaginella involven* Spring. *Chin Tradit Pat Med*. 2014;36:995-1000. https://doi.org/10.3969/j.issn.1001-1528.2014.05.024.
31 Swamy RC, Kunert O, Schühly W, et al. Structurally unique biflavonoids from *Selaginella chrysocaulos* and *Selaginella bryopteris*. *Chem Biodivers*. 2006;3(4):405-413. https://doi.org/10.1002/cbdv.200690044.
32 Seeger T, Geiger H, Zinsmeister HD, et al. Biflavonoids from the moss *Homalothecium lutescens*. *Phytochemistry*. 1993;34(1):295-296. https://doi.org/10.1016/S0031-9422(00)90823-9.
33 Long HP, Liu J, Xu PS, et al. Hypoglycemic flavonoids from *Selaginella tamariscina* (*P. Beauv*) Spring. *Phytochemistry*. 2022;195:113073. https://doi.org/10.1016/j.phytochem.2021.113073.
34 Tang T, Na Z, Xu YK. Chemical constituents from *Dysoxylum cauliflorum* (Meliaceae). *Nat Prod Res Dev*. 2012;24:777-779. https://doi.org/10.16333/j.1001-6880.2012.06.031.
35 Li D, Liu JP, Han X, et al. Chemical constituents of the whole plants of *Houttuynia cordata*. *Chem Nat Compd*. 2017;53(2):365-367. https://doi.org/10.1007/s10600-017-1991-6
36 Yang C, Wang JS, Kong LY. Chemical constituents from the needles of *Taxus canadensis*. *Chin J Nat Med*. 2011;9:188-190. https://doi.org/10.3724/SP.J.1009.2011.00188.
37 Aguilar MI, Romero MG, Chávez MI, et al. Biflavonoids isolated from *Selaginella lepidophylla* inhibit photosynthesis in spinach chloroplasts. *J Agr Food Chem*. 2008;56(16):6994-7000. https://doi.org/10.1021/jf8010432.
38 Gao XJ, Hu XL, Huang KW. Biflavonoid constituents from *Selaginella remotifolia* Spring. *Chin Pharm J*. 2016;51:1739-1743. https://doi.org/10.11669/cpj.2016.20.006.
39 Li S, Wang X, Wang G, et al. Ethyl acetate extract of *Selaginella doederleinii* Hieron induces cell autophagic death and apoptosis in colorectal cancer *via* PI3K-Akt-mTOR and AMPKα-signaling pathways. *Front Pharmacol*. 2020;11:565090. https://doi.org/10.3389/fphar.2020.565090.
40 Wang JZ, Li J, Zhao P, et al. Antitumor activities of ethyl acetate extracts from *Selaginella doederleinii* Hieron *in vitro* and *in vivo* and its possible mechanism. *Evid-Based Compl Alt*. 2015;2015(1):865714. https://doi.org/10.1155/2015/865714.
41 Webb AH, Gao BT, Goldsmith ZK, et al. Inhibition of MMP-2 and MMP-9 decreases cellular migration, and angiogenesis in *in vitro* models of retinoblastoma. *BMC Cancer*. 2017;17(1):434. https://doi.org/10.1186/s12885-017-3418-y.
42 Grimblat N, Zanardi MM, Sarotti AM. Beyond DP4: an improved probability for the stereochemical assignment of isomeric compounds using quantum chemical calculations of NMR shifts. *J Org Chem*. 2015;80(24):12526-12534. https://doi.org/10.1021/acs.joc.5b02396.
43 Grimblat N, Gavín JA, Hernández Daranas A, et al. Combining the power of *J* coupling and DP4 analysis on stereochemical assignments: the J-DP4 methods. *Org Lett*. 2019;21(11):4003-4007. https://doi.org/10.1021/acs.orglett.9b01193.